International Journal of Mechanical, Industrial and Aerospace Sciences
ISSN: 2517-9950
Vol:12, No:8, 2018

Influence of a Pulsatile Electroosmotic Flow on the Dispersivity of a Non-Reactive Solute through a Microcapillary

Jaime Muñoz, José Arcos, Oscar Bautista Federico Méndez

Abstract—The influence of a pulsatile electroosmotic flow (PEOF) at the rate of spread, or dispersivity, for a non-reactive solute released in a microcapillary with slippage at the boundary wall (modeled by the Navier-slip condition) is theoretically analyzed. Based on the flow velocity field developed under such conditions, the present study implements an analytical scheme of scaling known as the Theory of Homogenization, in order to obtain a mathematical expression for the dispersivity, valid at a large time scale where the initial transients have vanished and the solute spreads under the Taylor dispersion influence. Our results show the dispersivity is a function of a slip coefficient, the amplitude of the imposed electric field, the Debye length and the angular Reynolds number, highlighting the importance of the latter as an enhancement/detrimental factor on the dispersivity, which allows to promote the PEOF as a strong candidate for chemical species separation at lab-on-a-chip devices.

Keywords—Dispersivity, microcapillary, Navier-slip condition, pulsatile electroosmotic flow, Taylor dispersion, Theory of Homogenization.

I. Introduction

SINCE the classical work developed by Taylor [14] in the decade of 1950, which delivered the first description of the dispersivity as an enhanced diffusion process in the flow direction caused by the combined actions of axial convection and transversal diffusion across a tube, Taylor's dispersion theory has become fundamental at many studies related to the transport, separation and mixing of species with physiological, environmental or chemical applications.

In recent years, the dispersion mechanism has been of great relevance at transport processes for chemical species that govern the performance of labs-on-a-chip (LOCs) [1], [5], [12], [18], where the AC electroosmotic flow phenomenon (AC-driven EOF), by the other hand, has proven to be a valuable electrokinetic mechanism for mixing [13] and separation of mass species [7] due to the strong dependence among the oscillation frequency of the imposed electric field, the Debye length and the dispersivity. Until recently, the research work focused on the EOF dispersion has begun to consider the notable influence of the Navier-slip boundary condition [18], [21], which is capable of a notable enhancement at the electroosmotic velocity i.e., the Helmholtz-Smoluchowski velocity [15].

Despite the relevance of the AC-driven EOF referred above, the current EOF's dispersion studies including slippage at the wall assume a DC electric field [18], [21], so our study takes advantage of a particular AC-driven EOF: the pulsatile electroosmotic flow (PEOF), as an important mean for electroosmotic mass flow control and enhancement [4], [11], [19], [20], [22], in order to determine the dispersivity of a periodic PEOF with slippage at the wall, showing that such effects must be taken into consideration at for chemical species separation processes, one of the major fluidic issues to be performed on LOCs.

Jaime Muñoz is with the ESIME Zacatenco, Instituto Politécnico Nacional Av. Luis Enrique Erro S/N, Unidad Profesional Adolfo López Mateos, Zacatenco, Gustavo A. Madero, Ciudad de México 07738, Mexico (e-mail: ernesto8920@hotmail.com).

José Arcos and Oscar Bautista are with the ESIME Azcapotzalco, Instituto Politécnico Nacional Av. de las Granjas No. 682, Col. Santa Catarina, Azcapotzalco, Ciudad de México 02250, Mexico (e-mail: jarcos@ipn.mx, obautista@ipn.mx).

Federico Méndez is with the Universidad Nacional Autónoma de México, Coyoacan, Ciudad de México 04510, Mexico.

II. Problem Formulation

A schematic of the physical model under study is presented in Fig. 1. The dispersion of a non-reactive solute band along a microcapillary induced by a PEOF is considered. The radius is a, and its length is L. We define an aspect ratio, $\beta = a/L \ll 1$, that will be useful for our mathematical modeling. The electrical double layer (EDL) formed in the inner wall is quantified by the Debye length (λ_D) [8]. The PEOF is induced by applying a pulsating electric field, which dimensionless form is assumed to be,

$$E_x(t) = 1 + \xi \mathcal{I}m\left[\mathrm{e}^{it}\right], \tag{1}$$

where ω is the angular frequency, ξ is the amplitude of the electric field, $i = \sqrt{-1}$, $\mathcal{I}m[F]$ is the imaginary part of the complex quantity F and t is a dimensionless time normalized respect $1/\omega$. The resulting unidirectional periodic velocity field has been previously derived by Rojas *et al.* [11] considering slippage, in an dimensionless form as $u(r,t) = u_s(r) + \mathcal{I}m\left[u_\omega(r)\mathrm{e}^{it}\right]$, where $u_s(r)$ and $u_\omega(r)$ are the steady and oscillatory components of the velocity profile, respectively, they are defined as follows:

$$u_s(r) = 1 - \frac{I_0(\kappa r)}{I_0(\kappa)} + \kappa\delta\frac{I_1(\kappa)}{I_0(\kappa)}, \tag{2}$$

and

$$u_\omega(r) = \frac{\xi\kappa^2\left(\kappa^2 + iR_\omega\right)}{\left(\kappa^4 + R_\omega^2\right)I_0(\kappa)} \times \left[\frac{\left[I_0(\kappa) + \delta\kappa I_1(\kappa)\right]I_0(\sqrt{iR_\omega}r)}{I_0(\sqrt{iR_\omega}) + \delta\sqrt{iR_\omega}I_1(\sqrt{iR_\omega})} - I_0(\kappa r)\right], \tag{3}$$

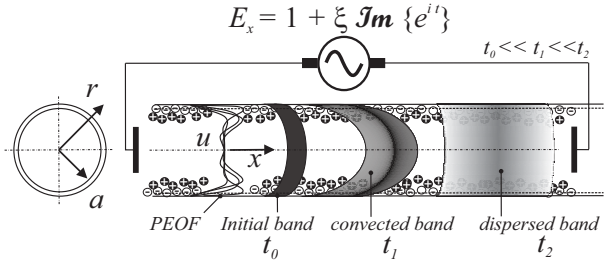

Fig. 1 Schematic diagram for a non-reactive solute under Taylor dispersion

with κ being the dimensionless electrokinetic parameter ($\kappa = a/\lambda_D$), R_ω is the angular Reynolds number [10], δ is the slip coefficient (defined as $\delta = \lambda_N/a$, with λ_N being the Navier length [6]). I_0 and I_1 are the zeroth- and first-order modified Bessel functions of the first kind, respectively.

Our objective is to analyze the transport of a neutral solute injected across the microcapillary at a large time scale, where the solute is axially propagated by the Taylor dispersion, this implies that the solute does not axially spread as fast as it would propagate radially, then we have a multiscale phenomenon with three time scales: a^2/D for the transversal diffusion, L/u_{HS} for the convection along L and L^2/D for the diffusion along L, with u_{HS} and D being the Helmholtz-Smoluchowski velocity and the molecular diffusion, respectively. We commence our analysis by considering the dimensionless convection-diffusion equation that governs the behavior of a solute in an isotropic medium, which is given by:

$$\frac{\partial C}{\partial t} + \beta Pe\; u(r,t)\frac{\partial C}{\partial x} = \beta^2\frac{\partial^2 C}{\partial x^2} + \frac{1}{r}\frac{\partial}{\partial r}\left(r\frac{\partial C}{\partial r}\right) \tag{4}$$

with

$$\frac{\partial C}{\partial r} = 0 \quad \text{at} \quad r = 0, 1. \tag{5}$$

The dimensionless concentration distribution is $C = \bar{C}/C_R$, where C_R is a reference concentration. $x = \bar{x}/L$, $t = \bar{t}D/a^2$ (please note that the quantities $\bar{C}$, $\bar{x}$ and $\bar{t}$ have physical units), also $Pe = u_{\text{HS}}a/D$ is the Péclet number [10], which is assumed to be of $\mathcal{O}(1)$. Next, we use the Homogenization Method [2], [16], [17] (an spatio-temporal averaging technique widely applied at multiscale phenomena analysis), in order to obtain a mathematical definition of the dispersivity, the detailed implementation of such technique is presented at Appendix A, here we summarize only its most relevant results:

• A set of ordinary differential equations named *canonical cell problems*:

$$\frac{1}{r}\frac{d}{dr}\left(r\frac{dB_s}{dr}\right) = \tilde{u}_s(r), \tag{6}$$

with

$$\frac{dB_s}{dr} = 0 \quad \text{at} \quad r = 0, 1, \tag{7}$$

and

$$\frac{1}{r}\frac{d}{dr}\left(r\frac{dB_\omega}{dr}\right) - iB_\omega = u_\omega(r), \tag{8}$$

with

$$\text{with} \quad \frac{dB_\omega}{dr} = 0 \quad \text{at} \quad r = 0, 1, \tag{9}$$

where $\tilde{u}_s = u_s(r) - \langle u_s(r)\rangle$, with $\langle u_s(r)\rangle$ being the mean velocity of u_s, defined as $2\int_0^1 r u_s dr$. Also, B_s and B_ω are functions of κ and R_ω, developed mainly as mathematical tools in order to calculate the dispersivity.

• A transport equation valid at the large time scale where the dispersion takes place:

$$\frac{\partial C_0}{\partial t_2} = \left[1 + Pe^2\left(\mathcal{D}_s + \mathcal{D}_\omega\right)\right]\frac{\partial^2 C_0}{\partial x^2}, \tag{10}$$

where C_0 is the leading order of C, as it has been considered in a form of perturbation series: $C = C_0 + \beta C_1 + \beta^2 C_2$, also, t_2 is a longitudinal diffusion time, with $\mathcal{D}_s$ and $\mathcal{D}_\omega$ being the steady and oscillatory components of the dispersivity, respectively. The effective dispersion coefficient or dispersivity is denoted by $\mathcal{D}$, with $\mathcal{D} = \mathcal{D}_s + \mathcal{D}_\omega$.

•A mathematical definition of the dispersivity, $\mathcal{D}$,

$$\mathcal{D} = -\left\{\langle \tilde{u}_s B_s\rangle + \frac{1}{2}\mathcal{R}e\langle u_\omega B_\omega^*\rangle\right\}, \tag{11}$$

with $\mathcal{D}_s = -\langle \tilde{u}_s B_s\rangle$, and $\mathcal{D}_\omega = -\frac{1}{2}\mathcal{R}e\langle u_\omega B_\omega^*\rangle$. The brackets $\langle\ \rangle$ represent a cross-sectional averaging procedure over the capillary transverse direction. Also, $\mathcal{R}e\,[F]$ is the real part of the complex quantity F and B_ω^* is the complex conjugate of B_ω.

III. Solution Methodology

By solving the boundary value problems (6) and (8), taking into account their corresponding boundary conditions and the PEOF velocity field (2)-(3), we have obtained a solution for B_s and B_ω, which are defined by,

$$B_s = \frac{1}{\kappa^2 I_0(\kappa)}\left[1 - I_0(\kappa r) + \frac{1}{2}\kappa r^2 I_1(\kappa) + \frac{\left(8-\kappa^2\right)I_1(\kappa) - 4\kappa}{4\kappa}\right] \tag{12}$$

$$\begin{aligned} B_\omega = \frac{\xi\Gamma_1}{2(\kappa^2 - i)(iR_\omega - i)J_1(i^{3/2})}\Big\{ & \sqrt{2}\kappa(1+i)(iR_\omega - i)I_1(\kappa)J_0(i^{3/2}r) \\ & - \sqrt{2}(1+i)\Gamma_2(\kappa^2 - i)\sqrt{iR_\omega}I_1(\sqrt{iR_\omega})J_0(i^{3/2}r) \\ & - 2iJ_1(i^{3/2})\left[(-1+R_\omega)I_0(\kappa r) + \Gamma_2(1+i\kappa^2)I_0(\sqrt{iR_\omega}r)\right]\Big\}, \end{aligned} \tag{13}$$

where J_0 and J_1 are the zeroth- and first-order Bessel function of the first kind, respectively. The functions Γ_1 and Γ_2 are explicitly shown at Appendix B.

Subsequently, (12) and (13) are substituted at (11) in order to obtain an explicit definition for $\mathcal{D}$ in terms of the parameters which control the PEOF hydrodynamic (κ, δ, R_ω, ξ). The stationary component $\mathcal{D}_s$ is given by,

$$\mathcal{D}_s = -\frac{1}{\kappa^2 I_0^2(\kappa)}\left[I_0^2(\kappa) - \left(\frac{3}{2} + \frac{8}{\kappa^2}\right)I_1^2(\kappa) + \frac{2}{\kappa}I_0(\kappa)I_1(\kappa)\right]. \tag{14}$$

By the other hand, the oscillatory component of the dispersivity is given by,

$$\mathcal{D}_\omega = -\frac{1}{2}\,\xi^2\,\mathcal{R}e\left\{\frac{\Gamma_1\Gamma_1^*\,\sum_{j=1}^{8}\Pi_j(R_\omega,\kappa,\delta)}{(\kappa^2+i)(-iR_\omega+i)J_1\left(\frac{-1-i}{\sqrt{2}}\right)}\right\}, \quad (15)$$

where Γ_1^* is the complex conjugate of Γ_1. Eq (15) has a singularity at $R_\omega = 1$, thus, by applying the L'Hopital rule we solve for D_ω as $R_\omega \to 1$, obtaining,

$$\lim_{R_\omega\to 1}\mathcal{D}_\omega = -\frac{1}{2}\,\xi^2\,\mathcal{R}e\left\{\sum_{j=1}^{7}\Psi_j(\kappa,\delta)\right\}. \quad (16)$$

Thus, $\mathcal{D}$ is defined by the sum of (14) and (15) for all $R_\omega > 0$, except at $R_\omega = 1$, where it is defined by the sum of (14) and (16). The functions $\Pi_j(R_\omega,\kappa,\delta)$ and $\Psi_j(\kappa,\delta)$ at (15) and (16), respectively, are completely defined at Appendix B.

IV. Results and Discussion

Our analytical expressions for the effective dispersivity ($\mathcal{D} = \mathcal{D}_s + \mathcal{D}_\omega$) have been derived as functions of the main parameters that control PEOF's hydrodynamics; in order to evaluate $\mathcal{D}$ for mass separation species, a suitable combination of values regarding the physical parameters used in experimental conditions [3], [9] was selected. Firstly, the expression $R_\omega = \Omega/Sc$ is substituted at (15) and (16), where $\Omega = a^2\omega/D$ represents a dimensionless frequency referred to the transverse mass diffusion time a^2/D and $Sc = \nu/D$ is the Schmidt number [8], which relates the time scale of the species diffusion to that of the viscous diffusion, then $\mathcal{D}$ is evaluated at different Sc. Considering a fixed kinematic viscosity for the carrier (water, $\sim \mathcal{O}(10^{-6})$ m^{2}s^{-1}), typical mass diffusivities of solutes in water, $D \sim \mathcal{O}(10^{-8}-10^{-9})$ m^{2}s^{-1}, in conjunction with typical radii ($10 \le a \le 100$ μm), then it is proposed three Sc values: $Sc = 100, 500,$ 2000, that describe different diffusive properties of three solutes. As ω must be kept below 1MHz in order to avoid kinematic instability [9], then the range $10^2 \le \Omega \le 10^5$ is considered in order to evaluate the dimensionless frequency dependency. Regarding the slip coefficient, a value $\delta = 0.1$, reported by experimental evidence [3], is considered; also, our analysis considers an electric field amplitude fixed at $\xi = 1.0$ with $\lambda_D \ll a$, in view of the latter condition, an EDL thickness with $\kappa = 100$ is proposed. Curves $\mathcal{D}$ vs Ω under all the circumstances referred above are shown at Fig. 2, such figure shows that $\mathcal{D}$ becomes increasingly constant from $\Omega \sim \mathcal{O}(10^2)$ to $\Omega \sim \mathcal{O}(10^3)$ as $Sc \to 2000$, and then evolves reaching a maximum value. Also, the molecular diffusion D or the Sc number does not exert any influence on the maxima of $\mathcal{D}$, however they determine the frequency Ω at which such maxima are achieved. Regardless the presence or not of slippage, for each Sc curve there is a specific range of frequencies where its dispersivity values are significantly larger than the others Sc curves; e.g., at Fig. 2 (b), with $\Omega \approx 1\times10^3$, 6×10^3 and 2.5×10^4, three different solutes with $Sc = 100$, 500 and 2000 provide the same maxima, however, as such maxima has been reached at different frequencies, three different regions around such frequencies are formed in

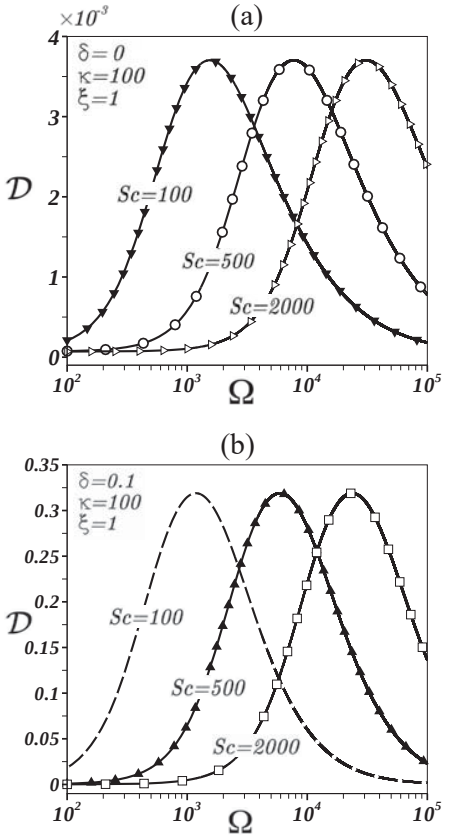

Fig. 2 Effective dispersivity $\mathcal{D}$ vs Ω for various Sc values ($Sc = 100$, 500, 2000), with $\kappa = 100$, $\xi = 1$ and two cases: (a) $\delta = 0$ and (b) $\delta = 0.1$. The points where $Sc = \Omega$ (or, equivalently, $R_\omega = 1$) were calculated considering (16) for the component $\mathcal{D}_\omega$

which a solute has a significantly large $\mathcal{D}$ in comparison the others Sc curves, this behavior favors the separation of solutes with different diffusive properties under a PEOF condition.

The change in the dominance of the dispersivity of one substance over another is determined by cross-over frequencies. Fig. 2 (b) shows that, when the slippage is present with $\delta = 0.1$ and $\kappa = 100$, the dispersivity $\mathcal{D}$ can be enhanced up to two orders of magnitude respect the no-slip case ($\delta = 0$) depicted at Fig. 2 (a).

V. Conclusion

There exists a strong coupling between the PEOF hydrodynamics and the rate of spread of a non-reactive immersed solute, in this context R_ω(or Ω) is a parameter that allows controlling $\mathcal{D}$, which results fundamental in order to properly separate chemical species immersed in such flow condition, as for certain values of this parameter, conditions have been found where there is a maximum of $\mathcal{D}$ or a detrimental behavior of it. Quantitative surprises have emerged from this study, as a slip condition with $\delta = 0.1$ enhances $\mathcal{D}$ up to two orders of magnitude respect the no-slip condition, with ξ being fixed and $\kappa \gg 1$, thus, the slippage at the boundary wall determines how efficiently the mass species separation

will be done and cannot be neglected at PEOF's micro-scale context.

APPENDIX

A. Homogenization Method

This appendix shows the development of the homogenization technique which has been made possible to derive a mathematical expression for the dispersivity of a non-reactive solute immersed in a PEOF with slippage at the boundary wall, presented at Section II.

Let's start by considering (4) which governs the transport of the solute under the PEOF condition:

$$\frac{\partial C}{\partial t}+\beta Pe\ u(r,t)\frac{\partial C}{\partial x}=\beta^2\frac{\partial^2 C}{\partial x^2}+\frac{1}{r}\frac{\partial}{\partial r}\left(r\frac{\partial C}{\partial r}\right)\ ;0<r<1 \tag{17}$$

As it was exposed at Section II, there exist different time scales associated with the solute propagation along the microcapillary, which describe the transversal diffusion time along a (a^2/D), the convective time along L (L/u_{HS}) and the longitudinal diffusion time along L (L^2/D), therefore, by introducing the following three time dimensionless coordinates:

$$t_0=t,\quad t_1=\beta t\quad\text{and}\quad t_2=\beta^2 t, \tag{18}$$

and proposing the perturbation series for the dimensionless concentration,

$$C=C_0+\beta C_1+\beta^2 C_2+..., \tag{19}$$

into (17), and after collecting terms of like powers in β, the following set of equations is obtained:

- the $\mathcal{O}\left(\beta^0\right)$ problem

At this order, the governing equation is given by,

$$\frac{1}{r}\frac{\partial}{\partial r}\left(r\frac{\partial C_0}{\partial r}\right)=0, \tag{20}$$

subject to the boundary conditions,

$$\frac{\partial C_0}{\partial r}=0\quad\text{at}\quad r=0,1. \tag{21}$$

Here, we have neglected the shortest time dependence for C_0 because we focus on the long behavior after the periodicity is completed. Accordingly, C_0 does not depend on r, and it is of the form,

$$C_0=C_0\left(x,t_1,t_2\right). \tag{22}$$

- the $\mathcal{O}\left(\beta\right)$ problem

The dimensionless convection-diffusion equation for C_1 is governed by the following problem:

$$\frac{\partial C_1}{\partial t_0}+\frac{\partial C_0}{\partial t_1}+Pe\left\{u_s+\ \mathcal{I}m\left[u_\omega \mathrm{e}^{it_0}\right]\right\}\frac{\partial C_0}{\partial x}=\frac{1}{r}\frac{\partial}{\partial r}\left(r\frac{\partial C_1}{\partial r}\right) \tag{23}$$

with the following boundary conditions,

$$\frac{\partial C_1}{\partial r}=0,\quad\text{at}\quad r=0,1. \tag{24}$$

- the $\mathcal{O}\left(\beta^2\right)$ problem

At this order, C_2 is governed by,

$$\frac{\partial C_2}{\partial t_0}+\frac{\partial C_1}{\partial t_1}+\frac{\partial C_0}{\partial t_2}+Pe\left\{u_s+\ \mathcal{I}m\left[u_\omega \mathrm{e}^{it_0}\right]\right\}\frac{\partial C_1}{\partial x}=\frac{\partial^2 C_0}{\partial x^2}+\frac{1}{r}\frac{\partial}{\partial r}\left(r\frac{\partial C_2}{\partial r}\right), \tag{25}$$

with the boundary conditions,

$$\frac{\partial C_2}{\partial r}=0;\quad r=0{,}1 \tag{26}$$

Considering that our interest is after the transients have died out, i.e., the periodic response, the time average during one period of oscillation of any function f is defined as, $\hat{f}=\frac{1}{2\pi}\int_0^{2\pi} f\ dt_0$.

Therefore, time-averaging (23) and (24) yields the following:

$$\frac{\partial C_0}{\partial t_1}+Pe\ u_s\frac{\partial C_0}{\partial x}=\frac{1}{r}\frac{\partial}{\partial r}\left(r\frac{\partial \hat{C}_1}{\partial r}\right) \tag{27}$$

with the following boundary conditions,

$$\frac{\partial \hat{C}_1}{\partial r}=0,\quad\text{at}\quad r=0,1. \tag{28}$$

The development of (27) continues. By defining the area average of a dimensionless quantity f as $\langle f\rangle=2\int_0^1 rf dr$, the cross-sectional average of (27) is given by,

$$\frac{\partial C_0}{\partial t_1}+Pe\ \langle u_s\rangle\frac{\partial C_0}{\partial x}=0. \tag{29}$$

Equation (29) stablishes that at the time scale t_1 the solute is convected by the PEOF. Subsequently, we subtract (29) from (23), thereby obtaining,

$$\frac{\partial C_1}{\partial t_0}+Pe\left\{\tilde{u}_s+\ \mathcal{I}m\left[u_\omega \mathrm{e}^{it_0}\right]\right\}\frac{\partial C_0}{\partial x}=\frac{1}{r}\frac{\partial}{\partial r}\left(r\frac{\partial C_1}{\partial r}\right), \tag{30}$$

where $\tilde{u}_s$ represents the deviation of the dimensionless velocity from its corresponding mean velocity, i.e., $\tilde{u}_s(r)=u_s(r)-\langle u_s(r)\rangle$.

Considering the linearity of (30), we can assume a solution for the variable C_1 as,

$$C_1=Pe\ \frac{\partial C_0}{\partial x}\left\{B_s(r)+\mathcal{I}m\left[B_\omega(r)\ e^{it_0}\right]\right\}. \tag{31}$$

Substituting (31) into (30) yields,

$$\mathcal{I}m\left(i\ B_\omega e^{it_0}\right)+\left[\tilde{u}_s(r)+\ \mathcal{I}m\left(u_\omega e^{it_0}\right)\right]=\frac{1}{r}\frac{d}{dr}\left(r\frac{dB_s}{dr}\right)+\mathcal{I}m\left[\frac{1}{r}\frac{d}{dr}\left(r\frac{dB_\omega}{dr}\right)e^{it_0}\right]. \tag{32}$$

B_s and B_ω are two functions which depend on the solutions of two boundary value problems, called *canonical cell problems*, such problems can been derived directly from (32) in conjuction with the boundary condition (24), and by solving them, it will be possible to obtain a constitutive relation for the dispersivity. Thus, the cell problems for the steady component B_s and for the oscillatory component B_ω are defined by,

$$\frac{1}{r}\frac{d}{dr}\left(r\frac{dB_s}{dr}\right)=\tilde{u}_s(r) \tag{33}$$

with the boundary conditions,

$$\frac{dB_s}{dr} = 0, \quad \text{at} \quad r = 0, 1. \tag{34}$$

For the oscillatory component B_ω we have,

$$\frac{1}{r}\frac{d}{dr}\left(r\frac{dB_\omega}{dr}\right) - i\ B_\omega = u_\omega(r), \tag{35}$$

with the boundary conditions,

$$\frac{dB_\omega}{dr} = 0, \quad \text{at} \quad r = 0, 1. \tag{36}$$

After defining these two cell problems, we continue developing (25), which corresponds to the $\mathcal{O}(\epsilon^2)$ problem, to obtain the dimensionless dispersivity coefficient $\mathcal{D}$ for the PEOF with slippage at the microcapillary wall. Substituting the definition of $\tilde{u}_s$, provided above, in conjunction with (31) into (25) leads to:

$$Pe^2\ \frac{\partial^2 C_0}{\partial x^2}\left[\tilde{u}_s + \langle u_s\rangle + \ \mathcal{I}m\left(u_\omega \mathrm{e}^{it_0}\right)\right] \times \left[B_s + \mathcal{I}m\left(B_\omega \mathrm{e}^{it_0}\right)\right] + \frac{\partial C_2}{\partial t_0} + \frac{\partial C_1}{\partial t_1} + \frac{\partial C_0}{\partial t_2} = \frac{\partial^2 C_0}{\partial x^2} + \frac{1}{r}\frac{\partial}{\partial r}\left(r\frac{\partial C_2}{\partial r}\right). \tag{37}$$

Taking (22), (29) and (31) into account, a useful expression for $\partial C_1/\partial t_1$ is as follows:

$$\frac{\partial C_1}{\partial t_1} = -Pe^2\ \langle u_s\rangle \frac{\partial^2 C_0}{\partial x^2}\left[B_s + \mathcal{I}m\left(B_\omega \mathrm{e}^{it_0}\right)\right]. \tag{38}$$

Introducing (38) into (37) leads to:

$$Pe^2 \frac{\partial^2 C_0}{\partial x^2}\left[\tilde{u}_s + \ \mathcal{I}m\left(u_\omega \mathrm{e}^{it_0}\right)\right] \times \left[B_s + \mathcal{I}m\left(B_\omega \mathrm{e}^{it_0}\right)\right] + \frac{\partial C_2}{\partial t_0} + \frac{\partial C_0}{\partial t_2} = \frac{\partial^2 C_0}{\partial x^2} + \frac{1}{r}\frac{\partial}{\partial r}\left(r\frac{\partial C_2}{\partial r}\right). \tag{39}$$

We now take the time average over a period regarding the shortest time scale, t_0, of (39). Special attention must be placed on the product $\left[\tilde{u}_s + \ \mathcal{I}m\left(u_\omega \mathrm{e}^{it_0}\right)\right] \times \left[B_s + \mathcal{I}m\left(B_\omega \mathrm{e}^{it_0}\right)\right]$ at the moment to obtain its short-time average, as it can be demonstrated that the period average of the product of the two harmonic functions $\eta = \mathcal{I}m\left(u_\omega \mathrm{e}^{it_0}\right)$ and $\tau = \mathcal{I}m\left(B_\omega \mathrm{e}^{it_0}\right)$ is given by $\hat{\eta\tau} = (1/2)\mathcal{R}e(u_\omega B_\omega^*)$, where $\mathcal{R}e[F]$ represents the real part of the complex quantity F and B_ω^* is the complex conjugate of B_ω. Thus, a differential equation for $\hat{C}_2$ is obtained in the form,

$$Pe^2 \frac{\partial^2 C_0}{\partial x^2}\left[\tilde{u}_s B_s + \frac{1}{2}\mathcal{R}e\left(u_\omega B_\omega^*\right)\right] + \frac{\partial C_0}{\partial t_2} = \frac{\partial^2 C_0}{\partial x^2} + \frac{1}{r}\frac{\partial}{\partial r}\left(r\frac{\partial \hat{C}_2}{\partial r}\right), \tag{40}$$

with the boundary conditions,

$$\frac{\partial \hat{C}_2}{\partial r} = 0, \quad \text{at} \quad r = 0, 1. \tag{41}$$

Subsequently, we obtain the cross-sectionally averaged form of (40), which is defined as,

$$\frac{\partial C_0}{\partial t_2} = \left[1 + Pe^2\left(\mathcal{D}_s + \mathcal{D}_\omega\right)\right]\frac{\partial^2 C_0}{\partial x^2}. \tag{42}$$

Equation (42) stablishes that at the long time scale t_2 the solute is transported by a combination of convective and radial diffusion propagation mechanisms known as Taylor dispersion. Here, the constitutive coefficient $1 + Pe^2\left(\mathcal{D}_s + \mathcal{D}_\omega\right)$ is sometimes referred as the effective diffusivity, denoted by E, and $\mathcal{D} = \mathcal{D}_s + \mathcal{D}_\omega$ is the dimensionless effective dispersion coefficient or dispersivity, which is composed of two parts: a steady dispersion coefficient that depends on the deviation from the mean velocity, $\mathcal{D}_s = -\langle \tilde{u}_s B_s\rangle$, and a oscillatory coefficient that depends on the periodic component of the velocity field, $\mathcal{D}_\omega = -\frac{1}{2}\mathcal{R}e\langle u_\omega B_\omega^*\rangle$. Therefore, the effective dispersivity is defined by,

$$\mathcal{D} = -\left\{\langle \tilde{U}_s B_s\rangle + \frac{1}{2}\mathcal{R}e\langle U_\omega B_\omega^*\rangle\right\}. \tag{43}$$

B. Function Components for the Oscillatory Dispersivity, $\mathcal{D}_\omega$

The parameters appearing at (12) and (13) are given by:

$$\Gamma_1 = \frac{\kappa^2\left(\kappa^2 + iR_\omega\right)}{\left(\kappa^4 + R_\omega^2\right) I_0(\kappa)} \tag{44}$$

and

$$\Gamma_2 = \frac{I_0(\kappa) + \delta\kappa I_1(\kappa)}{I_0(\sqrt{iR_\omega}) + \delta\sqrt{iR_\omega} I_1(\sqrt{iR_\omega})}. \tag{45}$$

The complex conjugates of such functions are defined by Γ_1^* and Γ_2^* which are as follows,

$$\Gamma_1^* = \frac{\kappa^2\left(\kappa^2 - iR_\omega\right)}{\left(\kappa^4 + R_\omega^2\right) I_0(\kappa)} \tag{46}$$

and

$$\Gamma_2^* = \frac{I_0(\kappa) + \delta\kappa I_1(\kappa)}{I_0\left(\frac{1-i}{\sqrt{2}}\sqrt{R_\omega}\right) + \frac{1-i}{\sqrt{2}}\delta\sqrt{R_\omega} I_1\left(\frac{1-i}{\sqrt{2}}\sqrt{R_\omega}\right)}. \tag{47}$$

Next, the parameters appearing at the general definition of dispersivity, i.e., (10), are given by:

$$\Pi_1 = \frac{\sqrt{2}\kappa}{1 + R_\omega}(1-i)(1-R_\omega) I_1(\kappa)\Gamma_2 \times \left[\sqrt{iR_\omega}\ J_0\left(\frac{-1-i}{\sqrt{2}}\right) I_1\left(\sqrt{iR_\omega}\right) + \left(\frac{-1-i}{\sqrt{2}}\right) J_1\left(\frac{-1-i}{\sqrt{2}}\right) I_0\left(\sqrt{iR_\omega}\right)\right] \tag{48}$$

$$\Pi_2 = \frac{(1-i)^2}{i(1+R_\omega)}(\kappa^2 + i)\Gamma_2\Gamma_2^*\sqrt{R_\omega}\ I_1\left(\frac{1-i}{\sqrt{2}}\sqrt{R_\omega}\right) \times \left[\sqrt{iR_\omega}\ J_0\left(\frac{-1-i}{\sqrt{2}}\right) I_1\left(\sqrt{iR_\omega}\right) + \left(\frac{-1-i}{\sqrt{2}}\right) J_1\left(\frac{-1-i}{\sqrt{2}}\right) I_0\left(\sqrt{iR_\omega}\right)\right] \tag{49}$$

$$\Pi_3 = \frac{\Gamma_2(R_\omega - 1)}{\kappa^2 - iR_\omega}\left[\kappa I_I(\kappa) I_0\left(\sqrt{iR_\omega}\right) - \sqrt{iR_\omega} I_0(\kappa) I_1\left(\sqrt{iR_\omega}\right)\right] \tag{50}$$

$$\Pi_4 = -\frac{\Gamma_2\Gamma_2^*}{2iR_\omega}\left(1 - i\kappa^2\right) \times \left[\left(\frac{1-i}{\sqrt{2}}\sqrt{R_\omega}\right)\ I_1\left(\frac{1-i}{\sqrt{2}}\sqrt{R_\omega}\right) I_0\left(\sqrt{iR_\omega}\right) - \sqrt{iR_\omega}\ I_0\left(\frac{1-i}{\sqrt{2}}\sqrt{R_\omega}\right) I_1\left(\sqrt{iR_\omega}\right)\right] \tag{51}$$

$$\Pi_5 = \frac{\sqrt{2}\kappa}{i+\kappa^2}(1-i)(i-iR_\omega)I_1(\kappa)\times \left[\kappa\, J_0\left(\frac{-1-i}{\sqrt{2}}\right) I_1(\kappa) + \left(\frac{-1-i}{\sqrt{2}}\right) J_1\left(\frac{-1-i}{\sqrt{2}}\right) I_0(\kappa)\right] \quad (52)$$

$$\Pi_6 = \Gamma_2^*(1-i)^2\sqrt{R_\omega} I_1\left(\frac{1-i}{\sqrt{2}}\sqrt{R_\omega}\right)\times \left[\kappa\, J_0\left(\frac{-1-i}{\sqrt{2}}\right) I_1(\kappa) + \left(\frac{-1-i}{\sqrt{2}}\right) J_1\left(\frac{-1-i}{\sqrt{2}}\right) I_0(\kappa)\right] \quad (53)$$

$$\Pi_7 = \frac{R_\omega - 1}{2}\left[I_0^2(\kappa) - I_1^2(\kappa)\right] \quad (54)$$

$$\Pi_8 = \frac{\Gamma_2^*\left(1-i\kappa^2\right)}{\kappa^2+iR_\omega}\times\left[\kappa\, I_0\left(\frac{1-i}{\sqrt{2}}\sqrt{R_\omega}\right) I_1(\kappa) - \left(\frac{1-i}{\sqrt{2}}\sqrt{R_\omega}\right) I_1\left(\frac{1-i}{\sqrt{2}}\sqrt{R_\omega}\right) I_0(\kappa)\right] \quad (55)$$

The parameters appearing at (11), which are related with the value of $\mathcal{D}_\omega$ as $R_\omega \to 1$ are defined by:

$$\Psi_1 = \frac{(1-i)\kappa^5 I_1(\kappa)\left[I_0(\kappa)+\delta\kappa I_1(\kappa)\right]}{\sqrt{2}(\kappa^2+i)J_1\left(\frac{-1-i}{\sqrt{2}}\right) I_0^2(\kappa)}\times \left[\frac{\sqrt{i}I_1(\sqrt{i})J_0\left(\frac{1+i}{\sqrt{2}}\right) + \left(\frac{1+i}{\sqrt{2}}\right) I_0(\sqrt{i})J_1\left(\frac{1+i}{\sqrt{2}}\right)}{i(\kappa^4+1)\left[I_0\left(\sqrt{i}\right)+\delta\sqrt{i}I_1\left(\sqrt{i}\right)\right]}\right] \quad (56)$$

$$\Psi_2 = -\frac{\sqrt{2}\kappa^4(1-i)(\kappa^2+i)\left[I_0(\kappa)+\delta\kappa I_1(\kappa)\right]^2}{(\kappa^2+i)J_1\left(\frac{-1-i}{\sqrt{2}}\right) I_0^2(\kappa)}\times \left\{\frac{\Lambda_2\Lambda_3}{\Lambda_1} + \frac{\Lambda_4}{\Lambda_1}\left(\frac{1-i}{\sqrt{2}}\right) I_1\left(\frac{1-i}{\sqrt{2}}\right)\right\} \quad (57)$$

$$\Psi_3 = -\frac{2\kappa^4\left[I_0(\kappa)+\delta\kappa I_1(\kappa)\right]}{(\kappa^2+i)I_0^2(\kappa)} \left\{\frac{\kappa I_0(\sqrt{i})I_1(\kappa) - (\sqrt{i})I_0(\kappa)I_1(\sqrt{i})}{(\kappa^2-i)(\kappa^4+1)\left[I_0\left(\sqrt{i}\right)+\delta\sqrt{i}I_1\left(\sqrt{i}\right)\right]}\right\} \quad (58)$$

$$\Psi_4 = \frac{\kappa^4\left[I_0(\kappa)+\delta\kappa I_1(\kappa)\right]^2}{\Lambda_5 I_0^2(\kappa)}\left\{\Lambda_6+\Lambda_7+\Lambda_8\right\} \quad (59)$$

$$\Psi_5 = -\frac{\sqrt{2}\kappa^5(1-i)I_1(\kappa)}{(\kappa^4+1)(\kappa^2+i)^2 J_1\left(\frac{-1-i}{\sqrt{2}}\right) I_0^2(\kappa)}\times \left\{\kappa J_0\left(\frac{-1-i}{\sqrt{2}}\right) I_1(\kappa) + \left(\frac{-1-i}{\sqrt{2}}\right) J_1\left(\frac{-1-i}{\sqrt{2}}\right) I_0(\kappa)\right\} \quad (60)$$

$$\Psi_6 = \frac{\kappa^4\left[I_0^2(\kappa)-I_1^2(\kappa)\right]}{I_0^2(\kappa)(\kappa^2+i)(\kappa^4+1)} \quad (61)$$

$$\Psi_7 = \frac{\kappa^4\left[I_0(\kappa)+\delta\kappa I_1(\kappa)\right]}{i(\kappa^2+i)I_0^2(\kappa)J_1\left(\frac{-1-i}{\sqrt{2}}\right)}\left(\frac{\Lambda_{10}-\Lambda_{11}}{\Lambda_9}\right) \quad (62)$$

The parameters Λ_j $(j = 1, \cdots, 11)$ through (57)-(62) are defined through (63)-(73) in the following forms:

$$\Lambda_1 = 2(\kappa^4+1)\left[I_0(\sqrt{i})+\delta\sqrt{i}I_1(\sqrt{i})\right] \left[I_0\left(\frac{1-i}{\sqrt{2}}\right) + \delta\left(\frac{1-i}{\sqrt{2}}\right) I_1\left(\frac{1-i}{\sqrt{2}}\right)\right] \quad (63)$$

$$\Lambda_2 = \frac{1}{2\sqrt{2}}(1-i)\, I_1\left(\frac{1-i}{\sqrt{2}}\right) - \left[\frac{i}{4} I_0\left(\frac{1-i}{\sqrt{2}}\right) + I_2\left(\frac{1-i}{\sqrt{2}}\right)\right] \quad (64)$$

$$\Lambda_3 = \sqrt{i}I_1(\sqrt{i})J_0(\sqrt{i}) + \sqrt{i}I_0(\sqrt{i})J_1(\sqrt{i}) \quad (65)$$

$$\Lambda_4 = \frac{iI_1(\sqrt{i})J_0(\sqrt{i})}{2\sqrt{i}} + \frac{iJ_0(\sqrt{i})}{4}\left[I_0(\sqrt{i})+I_2(\sqrt{i})\right] - \frac{1}{2\sqrt{2i}}(1-i)\, I_1(\sqrt{i})J_1(\sqrt{i}) \quad (66)$$

$$\Lambda_5 = -(\kappa^4+1)\left[I_0(\sqrt{i})+\delta\sqrt{i}I_1(\sqrt{i})\right] \left[I_0\left(\frac{1-i}{\sqrt{2}}\right) + \delta\left(\frac{1-i}{\sqrt{2}}\right) I_1\left(\frac{1-i}{\sqrt{2}}\right)\right] \quad (67)$$

$$\Lambda_6 = -\frac{\sqrt{i}}{2} I_0\left(\frac{1-i}{\sqrt{2}}\right) I_1(\sqrt{i}) + \left[\frac{1-i}{2\sqrt{2}} I_0(\sqrt{i}) I_1\left(\frac{1-i}{\sqrt{2}}\right)\right] \quad (68)$$

$$\Lambda_7 = \left[-\frac{1}{2}\sqrt{\frac{i}{2}}(1-i) + \frac{1}{2\sqrt{2i}}(1+i)\right] I_1(\sqrt{i}) I_1\left(\frac{1-i}{\sqrt{2}}\right) \quad (69)$$

$$\Lambda_8 = -\frac{i}{4}\left\{ I_0\left(\frac{1-i}{\sqrt{2}}\right)\left[I_0(\sqrt{i})+I_2(\sqrt{i})\right] + I_0(\sqrt{i})\left[I_0\left(\frac{1-i}{\sqrt{2}}\right) + I_2\left(\frac{1-i}{\sqrt{2}}\right)\right]\right\} \quad (70)$$

$$\Lambda_9 = -(\kappa^2+i)^2(\kappa^4+1)\left[I_0\left(\frac{1-i}{\sqrt{2}}\right) + \delta\left(\frac{1-i}{\sqrt{2}}\right) I_1\left(\frac{1-i}{\sqrt{2}}\right)\right] \quad (71)$$

$$\Lambda_{10} = \Theta_1\left\{\frac{1}{2\sqrt{2}}(1-i)(\kappa^2+i) I_1\left(\frac{1-i}{\sqrt{2}}\right) + \left(\frac{1+i}{\sqrt{2}}\right) I_1\left(\frac{1-i}{\sqrt{2}}\right) - \frac{i}{4}(\kappa^2+i)\left[I_0\left(\frac{1-i}{\sqrt{2}}\right) + I_2\left(\frac{1-i}{\sqrt{2}}\right)\right]\right\} \quad (72)$$

$$\Lambda_{11} = \Theta_2\left\{ -\frac{1}{2\sqrt{2}}(1-i)\, I_0(\kappa) I_1\left(\frac{1-i}{\sqrt{2}}\right) + \frac{\kappa}{2\sqrt{2}}(1-i)\, I_1(\kappa) I_1\left(\frac{1-i}{\sqrt{2}}\right) + \frac{i}{4} I_0(\kappa)\left[I_0\left(\frac{1-i}{\sqrt{2}}\right) + I_2\left(\frac{1-i}{\sqrt{2}}\right)\right]\right\}. \quad (73)$$

In (72) and (73), Θ_1 and Θ_2 have the following forms:

$$\Theta_1 = \sqrt{2}(1-i)(\kappa^2+i)\times \left[\kappa J_0\left(\frac{-1-i}{\sqrt{2}}\right) I_1(\kappa) + \left(\frac{-1-i}{\sqrt{2}}\right) J_1\left(\frac{-1-i}{\sqrt{2}}\right) I_0(\kappa)\right] \quad (74)$$

$$\Theta_2 = 2i(\kappa^2+i)(1-i\kappa^2) J_1\left(\frac{-1-i}{\sqrt{2}}\right) \quad (75)$$

ACKNOWLEDGMENT

This work was granted by the Programa Institucional de Formación de Investigadores by 2018222 from SIP-IPN, and the Fondo Sectorial de Investigación para la Educación from the Secretaria de Educación Pública- Consejo Nacional de Ciencia y Tecnología (No. CB-2013/220900). J. Muñoz acknowledges the support from CONACYT program for a Ph.D grant at SEPI-ESIME-IPN Zacatenco.

REFERENCES

[1] Stone H. A, Stroock A. D., and Ajdari A. Engineering flows in small devices: microfluidics toward a lab-on-a-chip. *Annu. Rev. Fluid Mech.*, 36:381–411, 2004.
[2] Mei C. C. and Vernescu B. *Homogenization methods for multiscale mechanics*. World scientific, 2010.
[3] Tretheway D. C. and Meinhart C. D. Apparent fluid slip at hydrophobic microchannel walls. *Phys. Fluids*, 14:9–12, 2002.
[4] J. Chakraborty, S. Ray, and S. Chakraborty. Role of streaming potential on pulsating mass flow rate control in combined electroosmotic and pressure-driven microfluidic devices. *Electrophoresis*, 33:419–425, 2012.
[5] Subhra Datta, , and Sandip Ghosal. Characterizing dispersion in microfluidic channels. *Lab Chip*, 9:2537–2550, 2009.
[6] Lauga E., Brenner M., and Stone H. *Microfluidics: The No-slip Boundary Condition*. Springer, Berlin Heidelberg, 2007.
[7] Huang H. F. and Lai C. L. Enhancement of mass transport and separation of species by oscillatory electroosmotic flows. *Proc. R. Soc. A.*, 462:2017–2038, 2006.
[8] Probstein R. F. *Physicochemical hydrodynamics: an introduction*. John Wiley and Sons, 1994.
[9] Green N. G., Ramos A., Gonzalez A., Morgan H., and Castellanos A. Fluid flow induced by nonuniform ac electric fields in electrolytes on microelectrodes. i. experimental measurements. *Phys. Rev.*, 61:4011–4018, 2000.
[10] Leal L. G. *Advanced transport phenomena*. Cambridge University Press, 2007.
[11] Rojas G., Arcos J., Peralta M., Méndez F., and Bautista O. Pulsatile electroosmotic flow in a microcapillary with the slip boundary condition. *Colloid Surf. A-Physicochem. Eng. Asp*, 513:57–65, 2017.
[12] Sandip Ghosal. Electrokinetic flow and dispersion in capillary electrophoresis. *Annu. Rev. Fluid Mech.*, 38:309–338, 2006.
[13] Oddy M. H., Santiago J. G., and Mikkelsen J. C. Electrokinetic instability micromixing. *Anal. Chem.*, 73:5822–5832, 2001.
[14] Taylor G. I. Dispersion of soluble matter in solvent flowing slowly through a tube. *Proc. R. Society A.*, 219:186–203, 1953.
[15] A. Matías, S. Sánchez, F. Méndez, and O. Bautista. Influence of slip wall effect on a non-isothermal electro-osmotic flow of a viscoelastic fluid. *Int. J. Therm. Sci.*, 98:352–363, 2015.
[16] C. C. Mei, J. L. Auriault, and C. O. Ng. Some applications of the homogenization theory. *Advances in Applied Mechanics*, 32:277–348, 1996.
[17] C. O. Ng. Dispersion in steady and oscillatory flows through a tube with reversible and irreversible wall reactions. *Proc. R. Soc. A*, 462:481–515, 2006.
[18] Ng C. O. and Zhou Q. Dispersion due to electroosmotic flow in a circular microchannel with slowly varying wall potential and hydrodynamic slippage. *Phys. Fluids.*, 24:112002, 2012.
[19] Suvadip Paul and Chiu-On Ng. Dispersion in electroosmotic flow generated by oscillatory electric field interacting with oscillatory wall potentials. *Microfluid Nanofluid*, 12:237–256, 2012.
[20] M. Peralta, J. Arcos, F. Méndez, and O Bautista. Oscillatory electroosmotic flow in a parallel- plate microchannel under asymmetric zeta potentials. *Fluid Dyn. Res.*, 49:035514, 2017.
[21] Zhou Q. and Ng C. O. Electro-osmotic dispersion in a circular tube with slip-stick striped wall qe11. *Fluid Dyn. Res.*, 47:015502, 2015.
[22] Chakraborty S. and Ray S. Mass flow-rate control through time periodic electro-osmotic flows in circular microchannels. *Phys. Fluids.*, 20(083602):1–11, 2008.